06-10 September 2021 EU PVSEC 2021 Lisbon, Portugal

INFLUENCE OF AN ACTIVE CRYSTAL COOLING DEVICE ON THE SHAPE OF THE PHASE BOUNDARY IN MONO INGOTS GROWN BY THE CZOCHRALSKI TECHNIQUE

F. Mosel[1], A.V. Denisov[1], K. Hess[1], B. Klipp[1], N. Sennova[1], C. Kranert[2], M. Trempa[2], C. Reimann[2], J. Friedrich[2]
[1] PVA Crystal Growing Sytems GmbH, Im Westpark 10-12, 35435 Wettenberg, Germany
[2]Fraunhofer-Institut für Integrierte Systeme IISB, Schottkystraße 10, 91058 Erlangen, Germany
e-mail: frank.mosel@pvatepla.com
tel: +49 64168690-125, fax: +49 64168690-822

Abstract
For the investigation of the influence of an active crystal cooling device on the shape of the crystallisation front, two different series of crystal growth experiments were carried out and interpreted with 2D numerical simulations. The deflections of the phase boundaries of the grown crystals were made visible by means of LPS-measurements and compared with the calculated interface shapes. In one of the two series, the influence of a certain crystal cooling element in connection with the growth configuration, especially the pull speed, was investigated. In the other series, the influence of different crystal cooling elements on the phase boundary at a certain growth rate was examined. Based on the heat flux balance at the crystallization front, the essential parameters for stable crystal growth conditions were evaluated.

Crystal growth equipment
The crystal growth experiments presented in this paper were performed in different growth configurations in a SC22 and a SC24/26 Czochralski-puller from PVA Crystal Growing Systems GmbH. The SC24/26 puller can be equipped optionally with a 24-inch or a 26-inch hotzone. The different crystal growth configurations are summarized in Tab.1.

growth configuration	Cz-puller type	crucible dimension [inch]	bottom heater	cooling element
Va	SC24	24	no	-
V1	SC22	22	no	A
V2	SC24/26	24, 26	yes	A
V2b	SC24	24	no	-
V3	SC26	26	yes	A, B, C, D, E

Tab.1: Main parameter of the different growth configurations

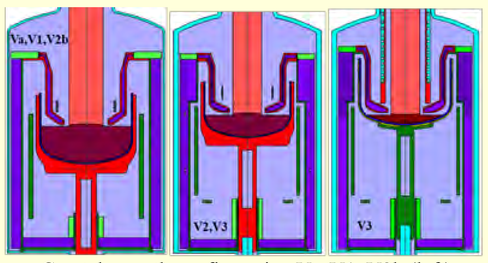

Crystal growth configuration Va, V1, V2b (left), V2, V3 (middle), V3 (right)

Crystal growth experiments
Two series of crystal growth experiments were realized:
Series A was performed from the standpoint of maximizing the average pull speed (Tab.2).
Series B was carried out (Tab.3) to investigate the influence of the different cooling elements (geometry and position) on the shape of the crystallization front.

ingot/growth configuration	average pull speed [mm/min]	crystal rotation [rpm]	crucible rotation [rpm]	gap [mm]	bottom heater	cooling element
CC212 Va	0.9	10	10	25	no	-
CC213 V2b	1.25	10	10	17	no	-
CC227 V2	1.8	10	6	17	yes	A
CC246 V3	1.6	10	6	17	yes	A
CC249 V1	1.2	10	10	25	no	A

Tab.2: Main growth parameters of Series A

ingot/growth configuration	average pull speed [mm/min]	crystal rotation [rpm]	crucible rotation [rpm]	gap [mm]	bottom heater	cooling device
CC262 V3	0.9	10	6	25	yes	E
CC263 V3	0.9	10	6	25	yes	B
CC265 V3	0.9	10	6	25	yes	B
CC266 V3	0.9	10	6	25	yes	D
CC267 V3	0.9	10	6	25	yes	C

Tab.3: Main growth parameters of Series B

Numerical simulation
All crystal growth runs were simulated using the commercially available FEM software CGSIM. The results presented here are derived from 2D simulations, which depict the axially symmetric formation of the calculated interface shape. To ensure the comparability between the growth experiments, the LPS measurements as well as the numerical simulations of the crystal growth conditions were all done at the growth stage of the body of 480 mm - 520 mm.

Characterization of the crystals
Vertically cut slices were prepared from all crystals and the solid liquid interface shapes were made visible by means of LPS measurements.

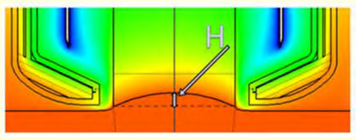

Sketch of a cooling element and the inner heat shield, **H** indicates the interface deflection

The shape of the phase boundary can be described by the deflection in the crystal center **H** and by the W-shape factor ϕ

$$\Phi[\%] = \frac{(\delta_{max} - \delta_{center})}{\delta_{max}}$$

Influence of the crystal cooling on the interface shape Series A
Calculated (blue line) and from LPS-measurement deduced interface shape (coloured thin lines)

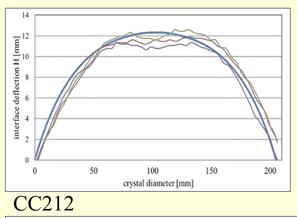

CC212

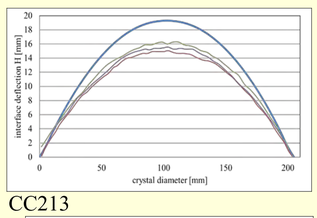

CC213

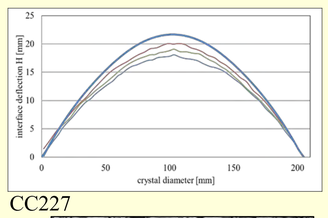

CC227

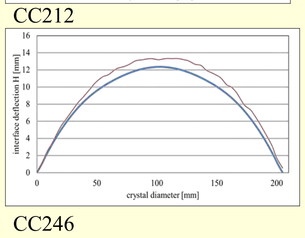

CC246

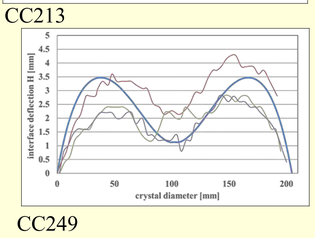

CC249

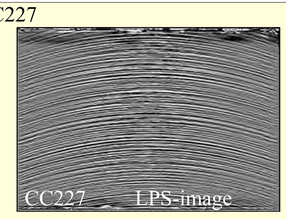

Influence of the crystal cooling on the interface shape Series B
Calculated (blue line) and from LPS-measurement deduced interface shape (coloured thin lines)

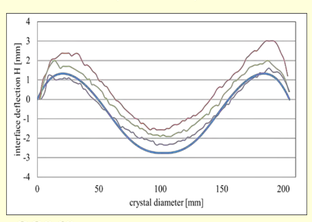

CC262

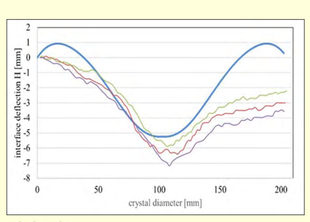

CC263

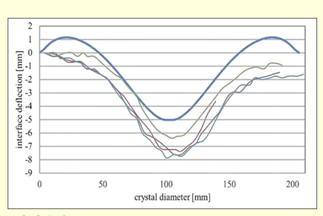

CC265

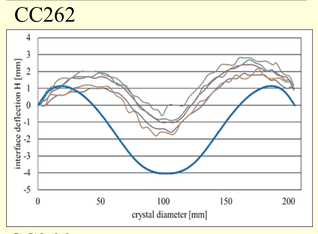

CC266

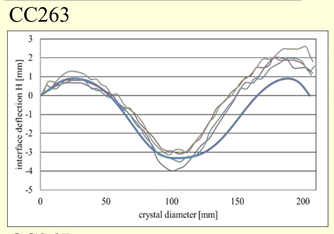

CC267

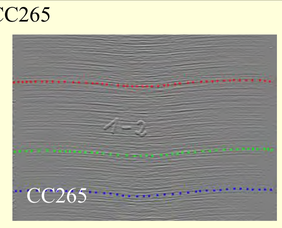

LPS-image

Ingot/growth configuration	active cooling element	average pull speed [mm/min]	deflection H [mm] measured	deflection H [mm] calculated	W-shape ϕ [%] measured	W-shape ϕ [%] calculated
CC212 Va	-	0.9	12	12	4	0
CC213 V2b	-	1.25	16	20	0	0
CC227 V2	A	1.8	20	22	0	0
CC246 V3	A	1.6	13	13	0	0
CC249 V1	A	1.2	1 to 2	1	35	68

Tab.4: Interface parameters of Series A

Ingot/growth configuration	active cooling element	average pull speed [mm/min]	deflection H [mm] measured	deflection H [mm] calculated	W-shape ϕ [%] measured	W-shape ϕ [%] calculated
CC262 V3	E	0.9	-2	-3	55	33
CC263 V3	B	0.9	-5 to -7	-5	0	15
CC265 V3	B	0.9	-6 to -8	-5	0	18
CC266 V3	D	0.9	-0.9 to -1.8	-4	60	25
CC267 V3	C	0.9	-3.1 to -4.1	-3	38	21

Tab.5: Interface parameters of Series B

Influence of the crystal cooling on the heat fluxes and temperature gradients at the interface of the growing crystal

Ingot/growth configuration	latent heat of fusion [W]	heat flow crystal [W]	heat flow melt [W]	G_l~Q/(Aλ) [K/cm]	G_s~Q/(Aλ) [K/cm]	G_{cr} [K/cm]
CC212 Va	2033	2990	960	4.8	45.3	3.74
CC213 V2b	2847	3470	625	3.1	52.6	1.34
CC249 V1	2727	4510	1780	8.9	68.3	7.89
CC246 V3	3639	4860	1220	6.1	73.6	5.63
CC227 V2	4102	4780	680	3.4	72.4	0.82

Tab.6: Thermal boundary conditions at the crystallization front of Series A

Ingot/growth configuration	latent heat of fusion [W]	heat flow crystal [W]	heat flow melt [W]	G_l~Q/(Aλ) [K/cm]	G_s~Q/(Aλ) [K/cm]	G_{cr} [K/cm]
CC262 V3	2053	3528	1475	7.3	53.5	7.75
CC263 V3	2046	3894	1848	9.2	59.0	9.46
CC265 V3	2047	3794	1746	8.7	57.5	8.40
CC266 V3	2043	3641	1604	8.0	55.2	7.52
CC267 V3	2057	3450	1400	7.0	52.3	6.40

Tab.7: Thermal boundary conditions at the crystallization front of Series B

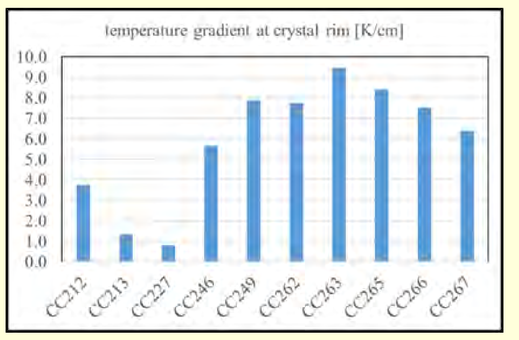

Calculated temperature gradient G_{cr} at the crystal rim

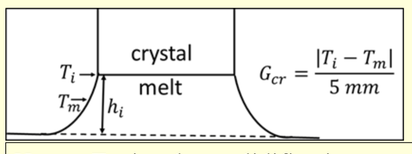

Here, T_i is the solidification temperature, T_m is the temperature on the melt meniscus at a distance of 5 mm from the crystal edge. T_m is therefore still within the thermal boundary layer, which corresponds to the meniscus height h_i (~ 6.9 mm). This key figure among others is used to judge the process stability.

Influence of active crystal cooling on the distribution of isotherms and von-Mises stresses in the growing crystal
Distribution of the von-Mises stresses [MPa] (left) and isotherms (right)

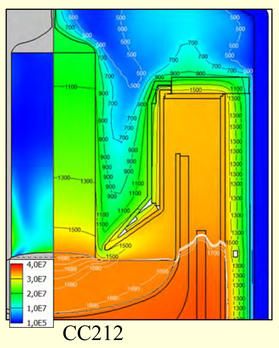
CC212

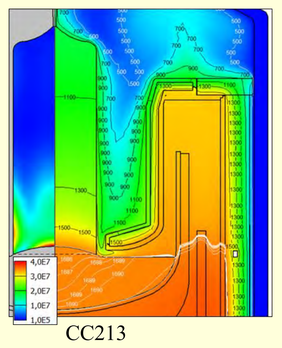
CC213

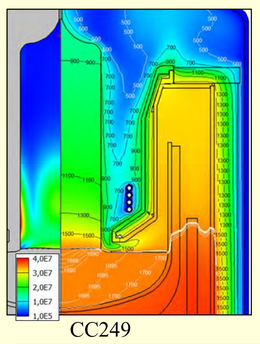
CC249

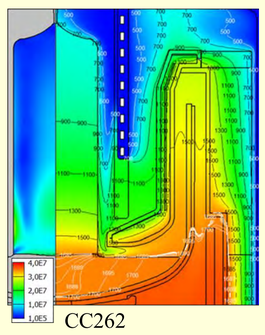
CC262

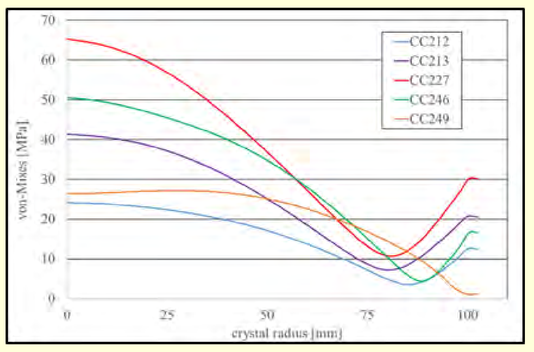

Von-Mises stress at the crystallisation front of Series A

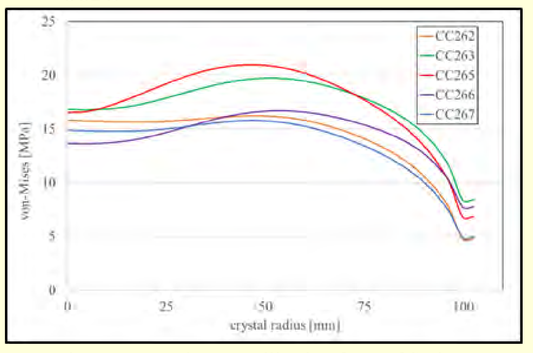

Von-Mises stress at the crystallisation front of Series B

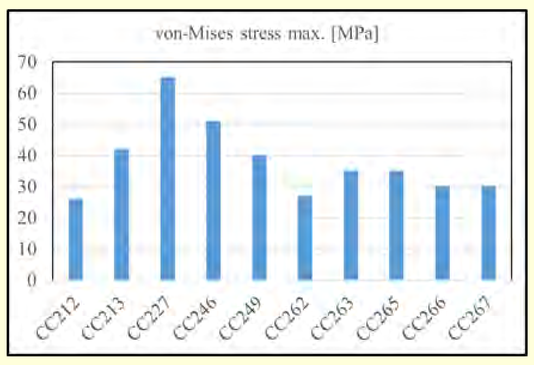

Calculated maximum von-Mises stress at a body length of 500 mm of the growing ingot

Conclusions
From the calculated heat fluxes at the phase boundary, a temperature gradient in the melt G_l should be > 3 K/cm and a temperature gradient at the crystal rim G_{cr} (melt meniscus) should be > 1 K/cm to establish stable growth conditions. At moderate growth rates the crystal cooling shows a clear impact on the shape of the interface. The axial temperature-time profile in the growing crystal can be effectively influenced by an active crystal cooling.

Influence of active crystal cooling on the axial temperature profile in the growing crystal

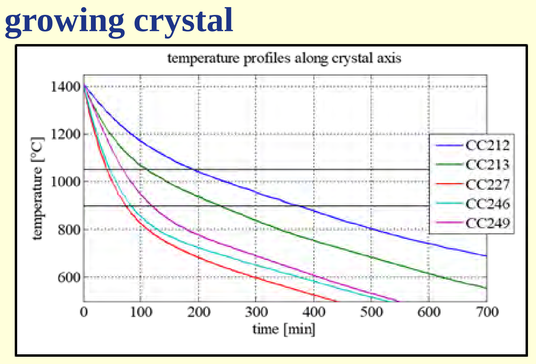

Calculated temperature profiles of Series A

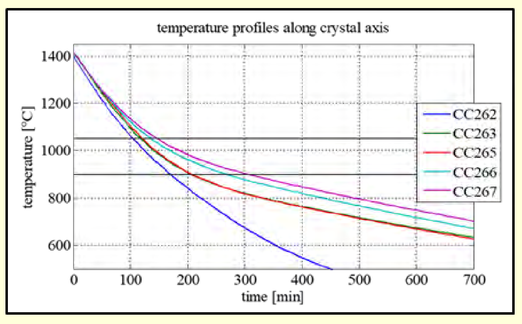

Calculated temperature profiles of Series B

Acknowledgements
This work was supported by the German Federal Ministry for Economic Affairs and Energy under contract numbers 0324281B and 0324357B.

Federal Ministry for Economic Affairs and Energy